INDERSCIENCE PUBLISHERS
Linking academia, business and industry through research

International Journal of Data Mining and Bioinformatics

ISSN online: 1748-5681 - ISSN print: 1748-5673
https://www.inderscience.com/ijdmb

Low resolution face recognition algorithm based on MB-LBP

Bin Fang

DOI: 10.1504/IJDMB.2023.10058131

Article History:

Received:	23 April 2023
Last revised:	23 May 2023
Accepted:	19 June 2023
Published online:	17 October 2023

Low resolution face recognition algorithm based on MB-LBP

Bin Fang

Department of Traffic Administration and Engineering,
Hunan Police Academy,
Changsha, 410138, China
Email: fsn201506@163.com

Abstract: Due to the low accuracy, poor stability, and long time consumption of current face recognition methods, a low resolution face recognition algorithm based on MB-LBP is proposed. Firstly, the facial edge image is processed through binarisation, followed by scale normalisation to accurately locate the face and the final cropped facial image. Then, segmented linear transformation is used for image enhancement processing. Finally, MB-LBP is used to extract features, and the Euclidean distance and cosine angle between the extracted feature vectors and the feature vectors extracted from the face database are calculated to achieve dual matching of facial images and achieve face recognition. The results show that the quality of the results obtained by this algorithm is good, with peak signal-to-noise ratio and recognition accuracy of 160 dB and 100%, variance of 0.01, and recognition time of 1.8 s, indicating that the algorithm proposed in this paper has reliable application performance.

Keywords: MB-LBP; low resolution; face recognition; binarisation; piecewise linear transformation.

Reference to this paper should be made as follows: Fang, B. (2023) 'Low resolution face recognition algorithm based on MB-LBP', *Int. J. Data Mining and Bioinformatics*, Vol. 27, No. 4, pp.279–296.

Biographical notes: Bin Fang received his Bachelor's and Master's in Computer Science and Technology from the School of Information Science and Engineering of Central South University in 2003 and 2009, respectively. He received his PhD in Transportation Equipment and Information Engineering from the School of Transportation Engineering of Central South University in 2016. He is currently an Associate Professor in the Department of Traffic Administration and Engineering of Hunan Police Academy. His research interests include intelligent transportation, traffic simulation and machine vision.

1 Introduction

With the continuous development of artificial intelligence technology, facial recognition technology has become an important application in fields such as security monitoring, financial payments, social entertainment, etc. However, in some scenarios, due to factors such as the installation position of the camera and lighting conditions, the collected facial images often have fewer pixels, resulting in low resolution facial images (Ge et al., 2020;

Gao et al., 2020). A low resolution image refers to an image with a relatively small number of pixels, and its display effect is usually blurry and unclear, with relatively few image details. On the contrary, high-resolution images refer to images with a relatively large number of pixels, and their display effects are usually clearer and more detailed. At present, the recognition effect for high-resolution facial images is good, but the accuracy for low resolution facial recognition is relatively low. Therefore, the research and development of low resolution facial recognition technology has very important practical significance.

Rouhsedaghat et al. (2021) proposed a low resolution face recognition method in resource constrained environments, constructing an interpretable non-parametric feature extraction submodel, using this model to extract facial features, and implementing face recognition based on the feature extraction results. The experimental results show that the model has the advantage of good generalisation ability, but there is a problem of long recognition time. Li et al. (2022) proposed a facial hallucination and recognition model for low resolution facial images based on feature mapping, which combines image feature loss and image content loss to jointly train the model. The experimental results show that the model can obtain comprehensive facial image features in recognition, but the accuracy of recognition results is low. Liang (2021) proposed an unrestricted face recognition algorithm based on transfer learning. First, improve the region extraction network of the fast RCNN algorithm, then process the unrestricted face image through the image enhancement algorithm, and finally realise face recognition through secondary transfer learning. The experimental results show that although the algorithm has a fast recognition speed, the peak signal-to-noise ratio (PSNR) of the recognition results is low and the variance is high.

Based on the existing problems of the above algorithms, this paper proposes a low resolution face recognition algorithm research based on multi-scale block local binary patterns (MB-LBP). Process the facial edge image through binarisation, then normalise the scale to accurately locate the face and the final cropped facial image, and then use segmented linear transformation to enhance the image. Finally, MB-LBP is used to extract features. Based on this, the Euclidean distance and cosine angle between the extracted feature vectors and the feature vectors extracted from the facial database are calculated accordingly to achieve accurate dual matching recognition of facial images, ensuring the accuracy of the final results and achieving facial recognition.

2 Overview and process of low resolution face recognition

Low resolution facial images refer to resolutions less than 32 × 32 low definition facial images, often captured by cameras under unconstrained conditions, often have many problems such as blurring, poor lighting conditions, high noise and occlusion (Li et al., 2020). Low resolution face recognition is the process of identifying the identity of such facial images. Currently, conventional face recognition methods typically perform less well than expected on low resolution facial images. Overall, low resolution facial images can be roughly divided into three categories:

1 Small size image: Refers to the small size of the face image to be recognised. In existing low resolution face recognition work, most of the work uses the size of the entire face image to refer to the face resolution. Traditional facial recognition

methods believe that even small-scale images can meet the needs of facial recognition tasks (Yang et al., 2020). However, most standard facial recognition methods have a resolution of less than 16 in facial images × at 16 o'clock, the recognition accuracy will significantly decrease.

2 Low quality image: Refers to an image that maintains its normal size, but suffers from severe loss of discriminative details in facial images due to poor shooting environment, inaccurate camera focus, and other issues. Using standard facial recognition methods for recognition cannot guarantee high recognition accuracy.

3 Images with both small-scale and low-quality issues mentioned above.

In real scenarios, facial images are generally captured by imaging devices such as cameras, and the quality of the image is determined by the lens and photosensitive devices of the imager. In practical application scenarios, the quality of imagers and photosensitive lenses is often relatively ordinary, so the captured image quality is also relatively low. Even if high-performance shooting equipment is used in certain scenes, such as crowded streets and dark alleys, various influencing factors have led to the generation of low resolution facial images due to the unconstrained nature of these scenes (Nadeem et al., 2021). The process of low resolution facial recognition is shown in Figure 1.

Figure 1 Face recognition process (see online version for colours)

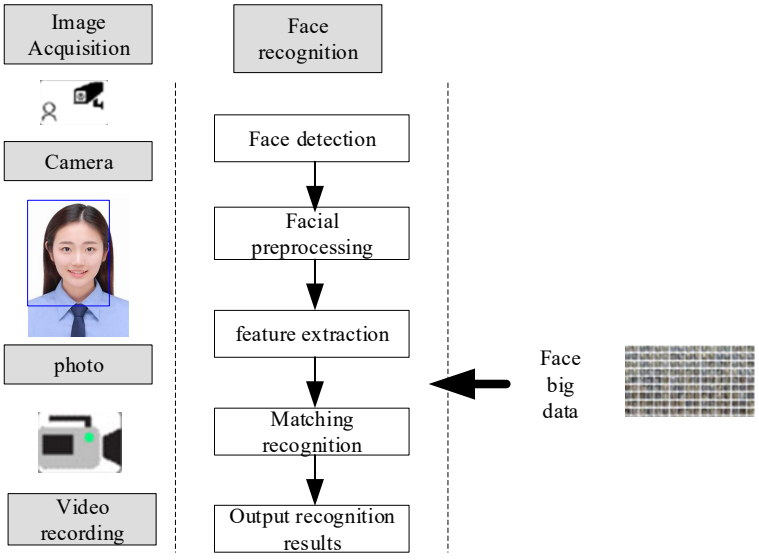

In face recognition engineering, image preprocessing, feature extraction, and matching recognition are the three steps that are currently more emphasised in low resolution face recognition. Preprocessing is a prerequisite for achieving accurate facial recognition, so the following will describe the above three steps.

3 Facial image preprocessing

After detecting a face, the edge image of the face is processed through binarisation to ensure correct normalisation of the face scale in order to accurately locate the face and the final cut face image. Finally, segmented linear transformation is used to enhance the image, laying the foundation for subsequent facial image matching and recognition.

3.1 Binarisation

In order to normalise the facial scale correctly, it is necessary to use binarisation to complete the processing of facial edge images. The main operation is to separate the contour from the background (Castellanos et al., 2021; Bardozzo et al., 2020). Finding a suitable threshold is the key to binary image processing. The maximum inter class variance method (Otsu) itself is an adaptive threshold determination method, so this method is chosen to complete the binarisation processing.

The Otsu method mainly segments the background and target in the image through the greyscale characteristics, in order to complete the main operational task of binarisation processing. Then, the probability of misclassification is determined by the variance between the background and the target after segmentation, which maximises the variance and minimises the misclassification probability. Among them, misclassification is defined as: the target is misclassified as the background or the background is misclassified as the target. The larger the variance, the smaller the probability of misclassification, which proves the better the processing effect. The specific operation process and related calculation formulas of its method are as follows.

Assuming the greyscale value at (x, y) is $m(x, y)$, where $m(x, y) \in [0, L-1]$ and L are the total number of greyscale levels in the image, and the total number of pixels is represented by N. Use m_i to represent the total number of a certain greyscale level, where $i = 0, 1, \ldots, L-1$. Next, use formula $p_i = m_i / N$ to calculate the probability of the occurrence of each greyscale level. According to the set threshold T, the image pixels can be divided into two regions: background A and target B, based on the greyscale level. Then, the probability of the occurrence of regions A and B is calculated, and the specific calculation expressions are as follows:

$$\rho_A = \sum_{i=0}^{T} p_i, \rho_B = \sum_{i=T+1}^{L-1} p_i \tag{1}$$

In the equation, $\rho_A + \rho_B = 1$, the mean values for categories A and B are:

$$\omega_A = \sum_{i=0}^{T} \frac{ip_i}{\rho_A}, \omega_B = \sum_{i=T+1}^{L-1} \frac{ip_i}{\rho_B} \tag{2}$$

The total mean of the image derived from equation (2) is:

$$\omega = \rho_A \omega_A + \rho_B \omega_B \tag{3}$$

It is easy to obtain the intra class variance of A and B from equations (1) and (2):

$$\delta_A^2 = \sum_{i=0}^{T} \frac{(1-\omega_A)^2 m_i}{\rho_A}, \delta_B^2 = \sum_{i=T+1}^{L-1} \frac{(1-\omega_B)^2 m_i}{\rho_B} \tag{4}$$

By using the above calculation formula, the intra class and inter class variances of the image can be obtained, and their calculation expressions are as follows:

$$\sigma_N^2 = \rho_A \delta_A^2 + \rho_B \delta_B^2, \sigma_J^2 = \rho_A (\omega_A - \omega)^2 + \rho_B (\omega_B - \omega)^2 \tag{5}$$

The total variance of the entire greyscale level is:

$$\sigma_T^2 = \sigma_N^2 + \sigma_J^2 \tag{6}$$

Because under normal circumstances, the variance of an image is always constant, the maximum inter class variance obtained from the above formula is equivalent to the minimum intra class variance. In order to achieve better segmentation between the target and the background, four Sobel edge detection can be performed on the original image first, and then an appropriate threshold T can be selected to complete the binarisation of the image. The results are shown in Figure 2.

Figure 2 Otsu binarisation of images and Otsu binarisation of edge images, (a) original image (b) binarisation effect image (c) binarisation effect image after edge detection

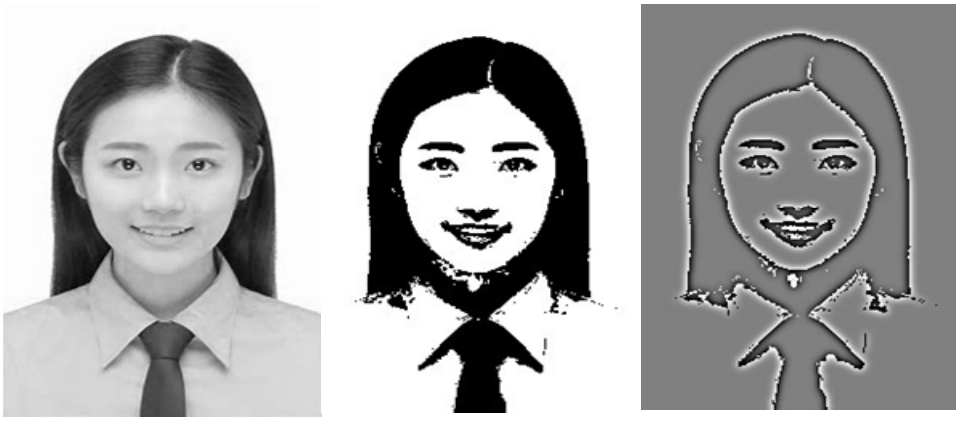

(a) (b) (c)

3.2 Scale normalisation

On the basis of the above content, to normalise the image scale, it is necessary to first locate the positions of the two eyes. Then, based on the distance between the two eyes, the traditional 'three courtyards and five eyes' method is used to reduce the image to a standard size, achieving facial localisation and the final facial image. This article uses the integral projection method for accurate binocular localisation on binary edge images (Chluba and Hart, 2020; Nasar et al., 2021). Assuming that $M(x, y)$ represents the binary image, the implementation process of scale normalisation is described as follows.

Firstly, the result graph c obtained from the above processing is represented by $M(x, y)$, and the vertical integration projection calculation is completed using the following formula (7):

$$V(x, y) = \sum_{y=y_1}^{y_2} M(x, y), y \in [y_1, y_2] \tag{7}$$

Similarly, the horizontal integral projection formula:

$$H(x, y) = \sum_{x=x_1}^{x_2} M(x, y), x \in [x_1, x_2] \tag{8}$$

From equations (7) and (8), it can be seen that the so-called integral projection is the sum of pixels on rows and columns of a binary image. The specific process is as follows.

Firstly, calculate the horizontal integral projection of the entire image, as shown in Figure 3.

Figure 3 Horizontal integral map corresponding to binary image (see online version for colours)

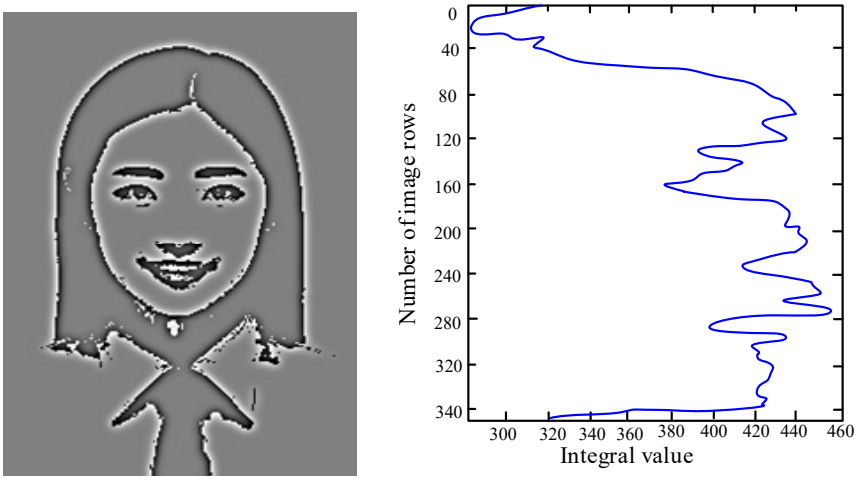

Figure 4 Vertical integral projection corresponding to eye template (see online version for colours)

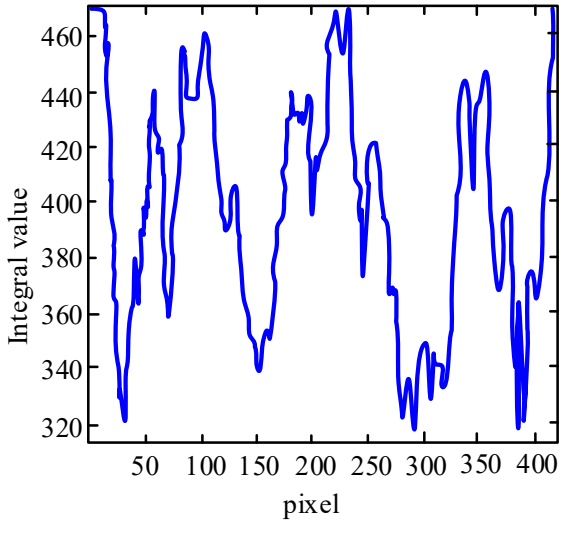

In Figure 3, the vertical axis represents the number of rows in the image, and the horizontal axis represents the integral value. From Figure 3, it can be seen that there are two minimum values within the pixel range [100, 400], corresponding to the approximate 'mouth' and 'eyes' of the human face, from which the abscissa of the human eye can be obtained. The vertical integration projection of the image in this interval is shown in Figure 4.

It is not difficult to see from Figure 4 that the integral projection has a maximum value within the pixel range [50, 350], corresponding to the 'bridge of the nose', and the coordinate at the minimum value between the left boundary and the 'bridge of the nose' is the vertical coordinate of the 'left eye'. Similarly, the vertical coordinate of the 'right eye' can be obtained. From this, the distance d between the eyes can be calculated.

Finally, according to the statement of 'three courtyards and five eyes', regions can be selected in both horizontal and vertical directions to ultimately determine the scale normalised facial regions. In the horizontal direction, connect the two eyes and take the distance d from the centre point of the line to the left and right directions respectively; in the vertical direction, the distance values are taken up and down, based on the position of the eyes. d / 2 and 3d / 2 are taken up and down, respectively, to obtain the scale up normalised face area. Figure 5 shows the accurate positioning of both eyes and the final cropped facial image.

Figure 5 'Standard face' under binocular localisation, (a) accurate binocular localisation (b) final standard face (see online version for colours)

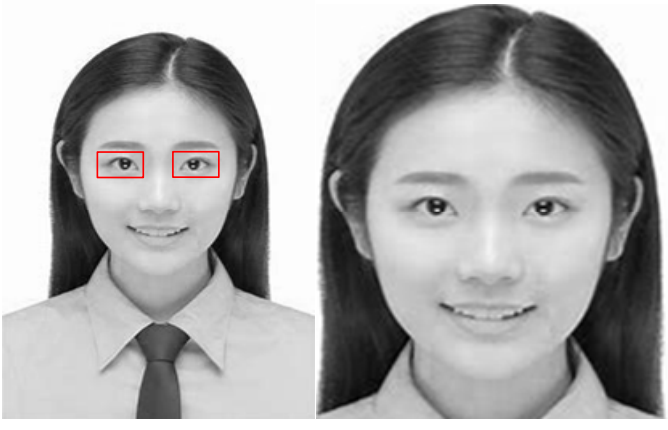

(a) (b)

3.3 Image enhancement

Due to the processing of the above stages, it often results in partial loss of image information, leading to misidentification. To solve this problem, image enhancement algorithms are usually used for corresponding image enhancement to compensate for lost information (Kansal and Tripathi, 2020; Yu et al., 2022; Saha et al., 2020). The segmented linear image enhancement method is one of the important means of image enhancement, belonging to the greyscale transformation method. The main task operation is to segment the greyscale interval of the image, and then use point operations to correct

the pixel greyscale to achieve enhancement. The enhanced image using this method is clearer and has more distinct features, so this article uses this method to achieve image enhancement (Bure et al., 2021; Dharejo et al., 2020). Taking three line segments as an example, the schematic diagram of their linear transformation is shown in Figure 6.

Figure 6 Schematic diagram of three segment linear transformation

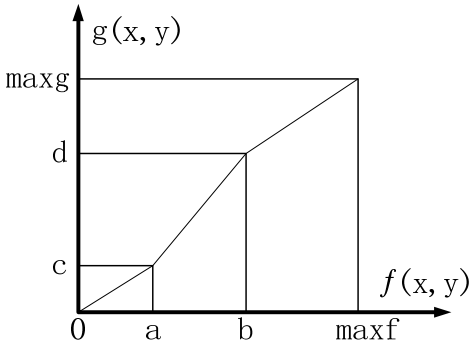

Figure 7 Facial image enhancement effect, (a) original image (b) after enhancement

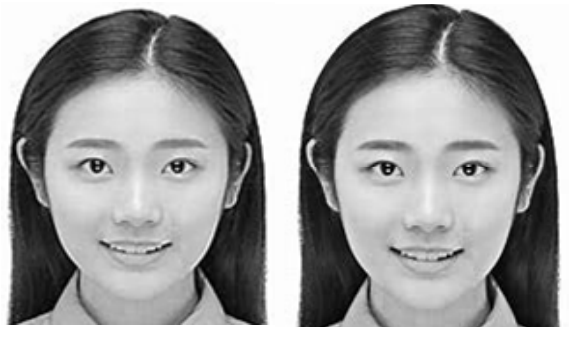

(a) (b)

In Figure 6, $f(x, y)$, $g(x, y)$ represents the greyscale levels of the original image and the transformed image, while max$f$ and max$g$ represent the maximum greyscale levels of the two images, respectively. Segmental linear transformation mainly achieves greyscale enhancement based on the greyscale details of stretched feature objects. Therefore, the greyscale range [a, b] to be enhanced in the above image is transformed into the expanded greyscale range [c, d] to achieve image enhancement. During this transformation process, the stretching and compression of the interval will result in the loss of its corresponding detailed information, but it will not have an adverse impact on the target recognition of the total weight. The transformation process can be represented by the following mathematical formula:

$$g(x, y)=\begin{cases}\dfrac{c}{a}f(x, y), & 0 \le f(x, y) < a \\ \dfrac{d-c}{b-a}\left[f(x, y)-a\right]-c, & a \le f(x, y) < b \\ \dfrac{\max g-d}{\max f-b}\left[f(x, y)+b\right]+d, & b \le f(x, y) < \max f\end{cases} \tag{9}$$

The parameter values of a, c, b, d, max$g$, and max$f$ in the above equation are: a = 20, c = 10, b = 180, d = 190 and max$g$ = max$f$ = 255.

Figure 7 shows an image and its effect after nonlinear enhancement. Figure 7(a) shows the degraded facial image used for recognition detected during the facial monitoring phase, and Figure 7(b) shows the normalised image to 92 × a face image with a size of 112 and greyed out, followed by segmented linear enhancement.

4 Low resolution facial recognition

To achieve accurate facial recognition, next, based on the above, feature extraction is performed on the enhanced image. In order to improve the integrity, accuracy, and speed of facial feature extraction, before and after feature extraction, halftone processing is performed on the images before and after addition, and then the MB-LBP algorithm is used to complete the feature extraction. Finally, in order to improve the accuracy of the recognition results, double matching recognition is performed using Euclidean distance and cosine angle. This process mainly calculates the Euclidean distance and cosine angle of the two extracted features, and sets a threshold to compare the calculated results with this threshold. If the Euclidean distance and cosine angle between the two features are less than the set threshold, then these two faces are the same person. The recognition results are output to complete face recognition.

Figure 8 Principle block diagram of error diffusion method

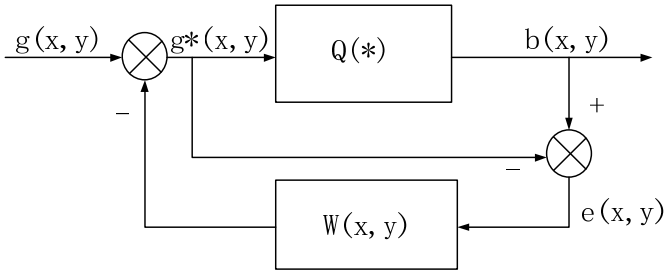

Digital halftone technology is an image reproduction technique that converts the original image into discrete halftone images such as black and white dots (Yu et al., 2021). Compared with traditional methods, digital halftone technology can enhance or weaken certain features in the image through different halftone algorithms, making the target features more obvious, thereby improving the accuracy and efficiency of subsequent facial recognition. Moreover, digital halftone technology preserves the original image features as much as possible while compressing data, so important information is not lost

in subsequent processing, which helps to improve the integrity of subsequent feature extraction.

Next, the error diffusion method is used to halftone the facial image, and the principle diagram is shown in Figure 8.

In Figure 8, $g(x, y)$, $g^*(x, y)$ is the input original image and the diffused input image respectively, and $b(x, y)$, $e(x, y)$ are the output binary image and quantisation error respectively. (x, y) represents each pixel in the image. The expression of the error diffusion process is as follows: first, add the original pixel value and the error spread here as the current input, as shown in equation (10); the output (0 or 1) obtained by thresholding the current input, as shown in equation (11); finally, the error values of the input and output are diffused to the unprocessed area according to a unique pattern, as shown in equation (12), to complete the halftone processing of the image.

$$g^*(x, y) = g(x, y) + \sum_{k,j} w(k, l)e(x-k, y-l) \tag{10}$$

$$b(x, y) = Q\left[g^*(x, y)\right] = Q\left[g(x, y)\right] + \sum_{k,j} w(k, l)e(x-k, y-l) \tag{11}$$

$$e(x, y) = b(x, y) - g^*(x, y) \tag{12}$$

In the formula, $w(k, l)$ represents the diffusion weight of the error diffusion filter at pixel point (k, l), and $Q[*]$ represents thresholding, which is usually taken as greyscale 128. The processed image is shown in Figure 9.

Figure 9 Halftone processing effect of facial images, (a) enhance image (b) halftone effect

(a) (b)

On the basis of the above, in order to effectively extract the texture information in the face image, enrich the feature expression and improve the accuracy of face recognition, MB-LBP feature extraction technology is used to extract features (Nan et al., 2022; Kong et al., 2021). This technology extracts the texture information between 'sub block regions' in the face image, and the extracted features are more abundant. Compared with traditional methods, MB-LBP can resist the influence of factors such as lighting, facial expressions, and posture, so it has stronger robustness for face recognition in different scenarios. At the same time, MB-LBP can extract texture features of facial images through multiple scales and directions, thereby enriching feature expression and improving the accuracy of facial recognition.

This technology mainly divides an image into multiple small blocks, and then divides the small blocks into regions. The average greyscale value is taken as the greyscale value of each region, which is compared with the greyscale values of the surrounding small regions to form a feature called MB-LBP. The calculation formula for MB-LBP feature extraction with R as the radius and P sampling points is as follows:

$$\text{MB-LBP}_{R,P} = \sum_{i=0}^{p-1} S(g_i)2^i \tag{13}$$

Among them, $S(g_i) = \begin{cases} 0, g_i = 0 \\ 1, g_i > 0 \end{cases}; 0 \le i \le P-1.$

In the MB-LBP calculation, the average value of each block must be less than 1, so in the histogram of the MB-LBP feature map, greyscale level 0 accounts for the largest proportion, as shown in Figure 10.

Figure 10 Statistics of greyscale histograms for MB-LBP feature extraction (see online version for colours)

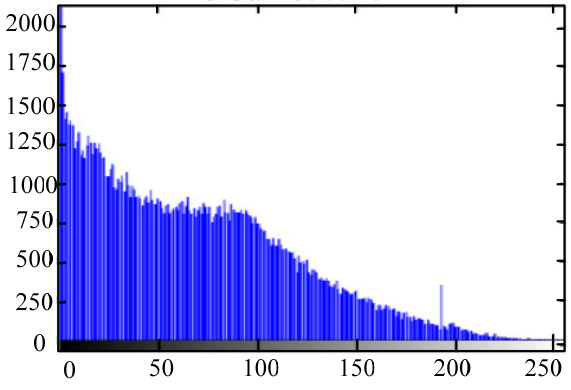

Figure 11 Euclidean distance versus cosine distance (see online version for colours)

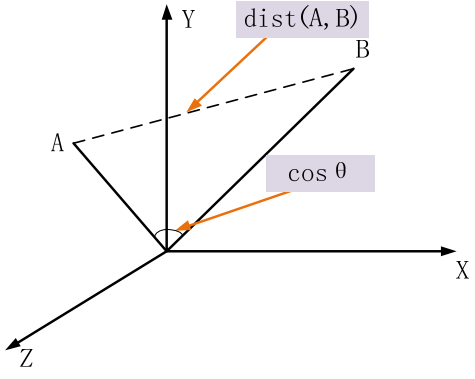

The feature vector extracted using the MB-LBP algorithm is defined as $x = x_1, x_2, \ldots, x_n$, and the facial feature vector in the face database is defined as $y = y_1, y_2, \ldots, y_n$. The Euclidean distance and cosine angle between the two are calculated to achieve dual

matching recognition of the facial image, ensuring the accuracy of the final output recognition results. Calculate the Euclidean distance and cosine angle between two feature vectors, as shown in Figure 11.

The calculation formula for its Euclidean distance is:

$$dist(x, y) = \sqrt{\sum_{k=1}^{n} \left(\frac{x_k - y_k}{s_k} \right)^2} \tag{14}$$

In the equation, s_k represents the difference coefficient between two feature vectors.

The cosine angle, also known as the similarity measure, is calculated using the formula:

$$d(\theta) = \frac{\sum_{k=1}^{n} x_k - y_k}{\sqrt{\sum_{k=1}^{n} (x_k)^2} \sqrt{\sum_{k=1}^{n} (y_k)^2}} \tag{15}$$

The similarity between two facial images is determined by the results obtained above. The smaller the distance result obtained, the greater the similarity measure. This indicates that the higher the similarity between the two feature vectors, the more similar the two facial images will be. Set the threshold to 1. If the results calculated by formulas (14) and (15) above are both less than the threshold, it indicates that these two faces are the same person. Output the recognition results to complete facial recognition and achieve the research of low resolution facial recognition algorithm based on MB-LBP.

5 Experimental analysis

5.1 Experimental plan design

5.1.1 Hardware environment

The experimental hardware environment is as follows.

The operating system is Windows 1064 bit, and the processor is Intel (R) Core (TM) i7-9700 CPU @ 3.00 GHz, 16 GB of memory, editor in Colorado, development language in Python, and development framework in PyTorch.

5.1.2 Low resolution facial dataset

This article uses the CASIA FaceV5 facial database training, which includes 500 photos of individuals, 5 of each person, and a total of 2,500 photos, including different age groups. Photo size: height 480, width 640, requires self partitioning of training and testing sets, self detection of faces from them, and saving. Use the CASIA-FaceV5 dataset with facial images numbered 0001–0400 as the training dataset, use the facial images numbered 0401–0500 as the test dataset, and use 50 of these 100 photos as 28 × 24.25 sheets 14 × 12.25 sheets 7 × 6 low resolution facial images are used as probes to detect faces from these 100 photos and save them as 112 × 96 high-resolution facial images as gallery.

5.1.3 Indicator settings

Four evaluation indicators are used to evaluate facial recognition algorithms, with specific descriptions as follows:

1 PSNR

PSNR is an objective indicator, measured in dB. The higher the PSNR value, the higher the quality of facial recognition.

$$PSNR = 10 * \log_{10}\left(\frac{MAX_I^2}{MSE}\right) = 20 * \log_{10}\left(\frac{MAX_I^2}{\sqrt{MSE}}\right) \tag{16}$$

In the formula, MAX_I and MSE represent the maximum value of pixels in the image and the mean square of the difference between the corresponding pixels between the two images.

2 Accuracy P

The proportion of the number of samples that can be accurately identified to the total test sample N is calculated as follows:

$$P = \frac{n}{N} \times 100\% \tag{17}$$

3 Variance S

The specific calculation formula for calculating the mean of multiple obtained experimental results as the corresponding dataset is as follows:

$$S = \frac{\sum_{i=1}^{m} (x_i - X)^2}{m} \tag{18}$$

In the formula, X is the average accuracy, x_i is the recognition accuracy of the i experiment, and M is the total number of experiments.

This indicator can measure the stability of the algorithm, and the smaller the value, the more stable the algorithm.

4 Test time t

This test was completed in MATLAB, and to record the test duration, the tic toc function was selected to record the code runtime of the algorithm. The running time of the code is equal to the recognition time of the algorithm.

5.2 Low resolution face recognition experiment

In order to verify the recognition accuracy and performance of the low resolution facial recognition algorithm proposed in this article, the algorithms in Rouhsedaghat et al. (2021), Li et al. (2022) and Liang (2021) were used as comparative algorithms for comparative testing with the proposed algorithm. Test and analyse the performance of four recognition algorithms: PSNR, recognition accuracy P, variance S, and algorithm time t.

5.2.1 PSNR test

Selecting 50 sheets from the dataset 28 × 24 low resolution facial images, using the proposed low resolution facial recognition algorithm, Rouhsedaghat et al. (2021) algorithm, Li et al. (2022), and Liang (2021) algorithm for facial recognition, The PSNR of the four algorithms is calculated according to formula (16), and the results are shown in Figure 12.

Figure 12 PSNR of face recognition results using different algorithms

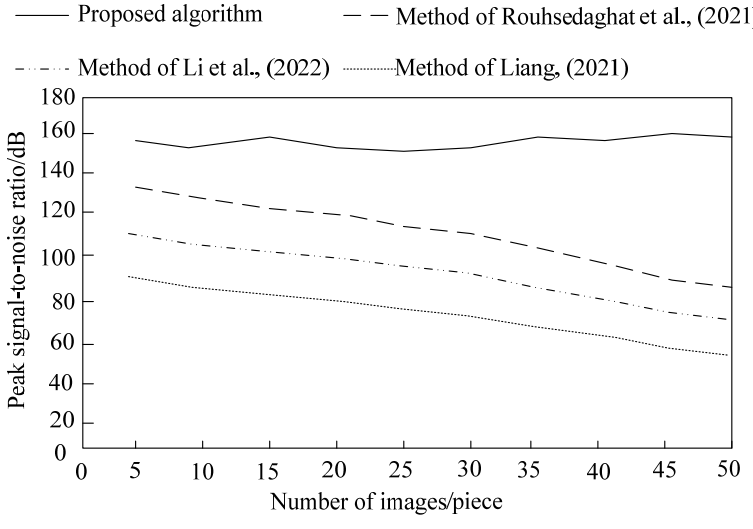

Analysing Figure 12, it can be seen that the PSNR of the proposed algorithm is higher than the other three algorithms. As the number of photos increases, its signal-to-noise ratio remains around 160 dB; the PSNR of the other three algorithms decreases with the increase of the number of photos. When the number of photos is 50, the PSNRs of the three low resolution facial recognition algorithms Rouhsedaghat et al. (2021), Li et al. (2022), and Liang (2021) are 100 dB, 80 dB and 60 dB, respectively. The proposed algorithm has a PSNR of 160 dB. Compared with the four low resolution facial recognition algorithms, the proposed algorithm has a higher PSNR, indicating that the proposed low resolution facial recognition algorithm produces higher quality recognition results and is more feasible.

5.2.2 Identification accuracy P test

Based on the above tests, calculate the recognition accuracy P of the four algorithms according to formula (17), and the results are shown in Figure 13.

According to Figure 13, it can be seen that the recognition accuracy of the proposed algorithm does not change with the number of photos, and is always 100%; the recognition accuracy of the other three algorithms changes with the increase of the number of photos. When the number of photos is 50, the recognition accuracy of the algorithms in Rouhsedaghat et al. (2021), Li et al. (2022), and Liang (2021) is 60%, 53% and 43%, respectively. The recognition accuracy of the proposed algorithm is 100%.

Compared with the four low resolution facial recognition algorithms, the proposed low resolution facial recognition algorithm has a higher recognition accuracy and greater reliability. This is because the proposed algorithm uses MB-LBP technology for facial recognition, which can resist the influence of factors such as lighting, facial expressions, and posture. Therefore, it has stronger robustness for facial recognition in different scenarios, and the technology can extract relatively complete facial image texture features, thereby improving the accuracy of facial recognition.

Figure 13 Recognition accuracy of four algorithms

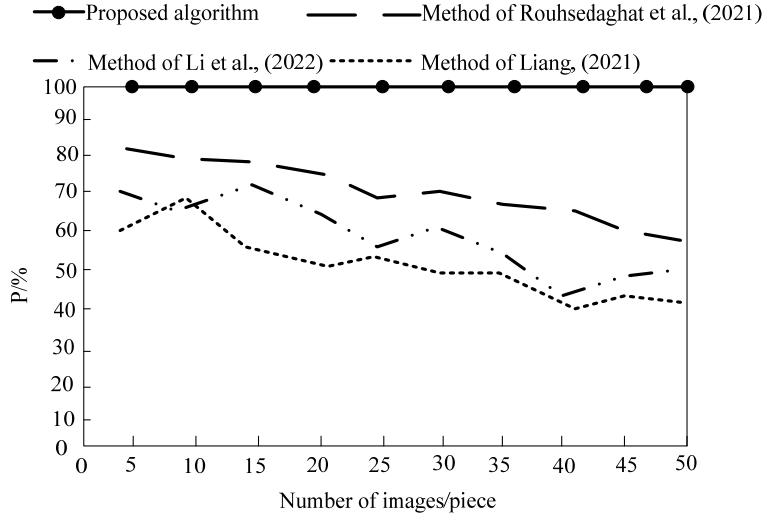

5.2.3 Variance S test

On the basis of the above experiments, 20 repeated experiments were conducted to calculate the variance *S* of the four algorithms according to formula (18). The results are shown in Table 1.

Table 1 Variance *S* results of four algorithms

Number of experiments / time	*Variance S*			
	Algorithm in this article	*Method of Rouhsedaghat et al. (2021)*	*Method of Li et al. (2022)*	*Method of Liang (2021)*
5	0.01	5.87	6.53	5.74
10	0.01	5.69	5.98	5.43
15	0.01	5.87	6.32	5.97
20	0.01	6.01	5.76	5.71

According to Table 1, the variance of the proposed algorithm does not change with the number of experiments, and its variance is always 0.01; the variance of the other three algorithms varies with the number of experiments, and according to formula (18), there is a certain relationship between their variance results and recognition accuracy. The algorithms in Rouhsedaghat et al. (2021), Li et al. (2022), and Liang (2021) have a

minimum variance of 5.69, 5.76, and 5.43 in 20 experiments, respectively. The variance of the proposed algorithm is always 0.01. Compared with the four low resolution facial recognition algorithms, the variance of the proposed low resolution facial recognition algorithm is smaller, indicating that the algorithm has stronger stability.

5.2.4 Algorithm time t test

On the basis of the above tests, the recognition time of the algorithm was recorded using the tic toc function in MATLAB, and the results are shown in Figure 14.

Figure 14 Recognition time of algorithm

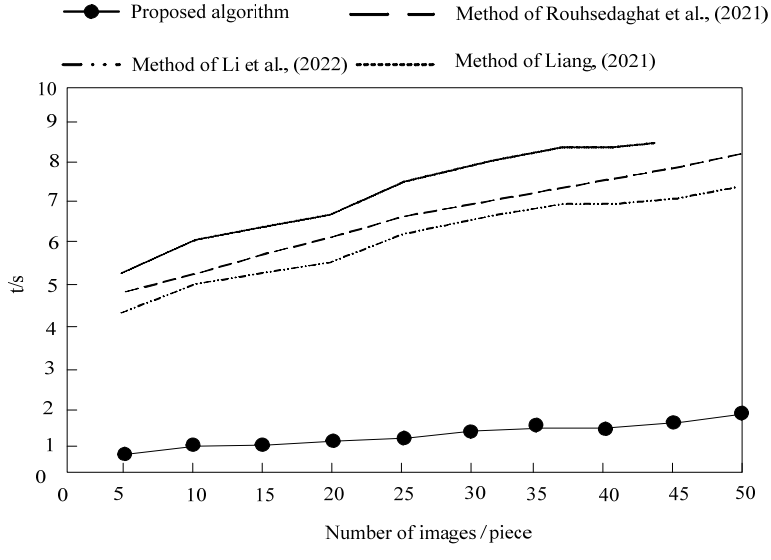

According to Figure 14, it can be seen that the recognition time of the four low resolution facial recognition algorithms increases with the number of photos. When the number of photos is 50, the recognition time of the proposed algorithm is 1.8 s. Compared with the four low resolution facial recognition algorithms, the proposed low resolution facial recognition algorithm has a shorter recognition time, indicating that the recognition speed of the algorithm is faster and more applicable. This is because the proposed algorithm uses digital halftone technology to process facial images before facial recognition. This technology can strengthen or weaken certain features in the image through different halftone algorithms, making the target features more obvious, thereby improving the efficiency of subsequent facial recognition.

6 Conclusions

In order to improve the accuracy and efficiency of facial recognition, a low resolution facial recognition algorithm based on MB-LBP is proposed. The main innovation points of this algorithm are as follows:

1 The use of MB-LBP technology for facial recognition can extract relatively complete facial image texture features, thereby improving the accuracy of facial recognition.

2 Before facial recognition, digital halftone technology is used to process facial images, which can strengthen or weaken certain features in the image, making the target features more obvious, thereby improving the efficiency of subsequent facial recognition.

3 The experimental results show that the algorithm achieves better quality results, with PSNR and recognition accuracy of 160 dB and 100%, variance of 0.01, and recognition time of 1.8 s. This indicates that the algorithm proposed in this paper has high recognition accuracy, strong stability, fast recognition speed, and reliable application performance.

In the future, research will focus on multimodal facial recognition, achieving more accurate and reliable facial recognition by integrating multiple information sources.

References

Bardozzo, F., De, B., Osa, L., Horanská, L. and Bustince, H. (2020) 'Sugeno integral generalization applied to improve adaptive image binarization', *Information Fusion*, Vol. 68, No. 9, pp.37–45.

Bure, L, Sato, Y. and Pautz, A. (2021) 'Piecewise linear interface-capturing volume-of-fluid method in axisymmetric cylindrical coordinates', *Journal of Computational Physics*, Vol. 436, No. 1, pp.1129–1138.

Castellanos, F.J., Gallego, A.J. and Calvo-Zaragoza, J. (2021) 'Unsupervised neural domain adaptation for document image binarization', *Pattern Recognition*, Vol. 119, No. 4, pp.108–119.

Chluba, J. and Hart, L. (2020) 'Improved model-independent constraints on the recombination era and development of a direct projection method', *Monthly Notices of the Royal Astronomical Society*, Vol. 495, No. 4, pp.4210–4226.

Dharejo, F.A., Zhou, Y., Deeba, F., Jatoi, M.A. and Wang, X. (2020) 'A remote-sensing image enhancement algorithm based on patch-wise dark channel prior and histogram equalisation with colour correction', *IET Image Processing*, Vol. 15, No. 3, pp.47–56.

Gao, G., Yu, Y.B., Yang, M.D., Chang, H.E., Huang, P.A. and Yue, D.A. (2020) 'Cross-resolution face recognition with pose variations via multilayer locality-constrained structural orthogonal procrustes regression', *Information Sciences*, Vol. 506, No. 12, pp.19–36.

Ge, S., Zhao, S., Li, C., Zhang, Y. and Li, J. (2020) 'Efficient low-resolution face recognition via bridge distillation', *IEEE Transactions on Image Processing*, Vol. 23, No. 9, pp.11–19.

Kansal, S. and Tripathi, R.K. (2020) 'New adaptive histogram equalisation heuristic approach for contrast enhancement', *IET Image Processing*, Vol. 14, No. 6, pp.1110–1119.

Kong, F., Zhao, S., Li, Y. and Li, D. (2021) 'End-to-end multispectral image compression framework based on adaptive multiscale feature extraction', *Journal of Electronic Imaging*, Vol. 30, No. 1, pp.1–19.

Li, H., Li, M., Liu, Q., Swindlehurst, A.L. and Swindlehurst, L. (2020) 'Dynamic hybrid beamforming with low-resolution PSs for wideband mmWave MIMO-OFDM systems', *IEEE Journal on Selected Areas in Communications*, Vol. 38, No. 9, pp.2168–2181.

Li, S., Liu, Z., Wu, D., Huo, H., Wang, H. and Zhang, K. (2022) 'Low-resolution face recognition based on feature-mapping face hallucination', *Computers and Electrical Engineering*, Vol. 101, No. 9, pp.3–12.

Liang, Z. (2021) 'Unrestricted face recognition algorithm based on transfer learning on self-pickup cabinet', *Mathematical Problems in Engineering*, Vol. 25, No. 17, pp.1–12.

Nadeem, U., Shah, S.A.A., Bennamoun, M., Togneri, R. and Sohel, F. (2021) 'Real time surveillance for low resolution and limited data scenarios: an image set classification approach', *Information Sciences*, Vol. 580, No. 2, pp.578–597.

Nan, F., Jing, W., Tian, F., Zhang, J., Chao, K.M., Hong, Z. and Zheng, Q. (2022) 'Feature super-resolution based facial expression recognition for multi-scale low-resolution images', *Knowledge-based Systems*, Vol. 236, No. 25, pp.107–115.

Nasar, A.M.A., Fourtakas, G., Lind, S.J., King, J.R.C. and Stansby, P.K. (2021) 'High-order consistent SPH with the pressure projection method in 2-D and 3-D', *Journal of Computational Physics*, Vol. 444, No. 3, pp.1563–1573.

Rouhsedaghat, M., Wang, Y., Hu, S., You, S. and Kuo, C.C.J. (2021) 'Low-resolution face recognition in resource-constrained environments', *Pattern Recognition Letters*, Vol. 149, No. 10, pp.193–199.

Saha, R., Banik, P.P., Gupta, S.S. and Kim, K.D. (2020) 'Combining highlight removal and low-light image enhancement technique for HDR-like image generation', *IET Image Processing*, Vol. 14, No. 9, pp.1851–1861.

Yang, Y., Wu, J., Wang, M., Wang, Q. and Chen, K.P. (2020) 'Fast demodulation of fiber bragg grating wavelength from low-resolution spectral measurements using Buneman frequency estimation', *Journal of Lightwave Technology*, Vol. 58, No. 6, pp.5142–5148.

Yu, M., Yin, X., Liu, W. and Lu, W. (2021) 'Secure halftone image steganography based on density preserving and distortion fusion', *Signal Processing*, Vol. 188, No. 11, pp.108227–108239.

Yu, N., Li, J. and Hua, Z. (2022) 'LBP-based progressive feature aggregation network for low-light image enhancement', *IET Image Processing*, Vol. 16, No. 2, pp.535–553.